PUBLICATION V

Modelling anelastic contribution to nuclear fuel cladding creep and stress relaxation

Journal of Nuclear Materials, **465**, 34–41.

Journal of Nuclear Materials 465 (2015) 34–41

Contents lists available at ScienceDirect

Journal of Nuclear Materials

journal homepage: www.elsevier.com/locate/jnucmat

Modelling anelastic contribution to nuclear fuel cladding creep and stress relaxation

Ville Tulkki*, Timo Ikonen

VTT Technical Research Centre of Finland Ltd, P.O.Box 1000, 02044, VTT, Finland

ARTICLE INFO

Article history:
Received 24 January 2015
Received in revised form
10 April 2015
Accepted 25 April 2015
Available online 3 June 2015

Keywords:
Zircaloy-4
Cladding
Stress relaxation
Creep
Anelastic
Viscoelastic
Modelling

ABSTRACT

In fuel behaviour modelling accurate description of the cladding mechanical response is important for both operational and safety considerations. While accuracy is desired, a certain level of simplicity is needed as both computational resources and detailed information on properties of particular cladding may be limited. Most models currently used in the integral codes divide the mechanical response into elastic and viscoplastic contributions. These have difficulties in describing both creep and stress relaxation, and often separate models for the two phenomena are used.

In this paper we implement anelastic contribution to the cladding mechanical model, thus enabling consistent modelling of both creep and stress relaxation. We show that the model based on assumption of viscoelastic behaviour can be used to explain several experimental observations in transient situations and compare the model to published set of creep and stress relaxation experiments performed on similar samples. Based on the analysis presented we argue that the inclusion of anelastic contribution to the cladding mechanical models provides a way to improve the simulation of cladding behaviour during operational transients.

1. Introduction

The cladding of a fuel rod both contains the radioactive fission products and protects the fuel pellets from the cooling water. As such, the integrity of the cladding tube is of utmost importance. During its reactor life, the cladding tube is first under a pressure differential at elevated temperatures and under irradiation, and creeps inwards. The rate of this inward creep determines in part the time of hard contact between the fuel pellets and the cladding wall as well as influences the heat conduction across the gas gap. After a hard contact between the pellet and the cladding wall the pellets push the cladding outward as they expand. At high burnup the rod internal overpressure may even push the cladding to creep faster than the fuel pellet swells. Ergo, at different times the cladding wall is either freestanding under a pressure differential, a case where creep deformation is of interest, or experiences forced displacement with unknown stress that needs to be solved.

Fuel behaviour analysis is commonly performed with integral codes utilizing separate models to describe various phenomena. The number of individual models is large and the number of required fuel rod simulations may rise to hundreds of thousands depending on the application. As such, a simple and practical approach to modelling cladding creep and stress relaxation is needed. Conventionally creep models are derived from experiments conducted with internally pressurized tubes. The models have been used utilizing strain hardening law to take into account the cladding behaviour during alternating stresses. However, the conventional strain hardening law cannot be used to describe creep response to load drops or reversals [1–4], and this is also an issue modelling stress relaxation where the stress is constantly decreasing. Yet in order to model the fuel rod cladding mechanical behaviour during its whole reactor life, the model needs to be able to describe also the stress relaxation behaviour. While strain hardening law has its deficiencies it has been widely adopted in fuel behaviour codes in part due to its simplicity. In order for the alternative approach to replace the established strain hardening law it also needs to retain simplicity and implementability of the old approach.

In our previous work we have introduced an empirical model based on the viscoelastic theory that is capable of describing the observed creep response to transient stresses [5,6]. Viscoelastic models should be able to describe both the creep and the stress

* Corresponding author.
E-mail address: ville.tulkki@vtt.fi (V. Tulkki).

http://dx.doi.org/10.1016/j.jnucmat.2015.04.056
0022-3115/

relaxation behaviour of the materials, at least for small deformations [7]. Therefore assessing the model capability for zirconium alloy stress relaxation is of interest. In this paper we investigate the time evolution of cladding transient response, construct a viscoelastic model and both qualitatively and quantitatively investigate the model behaviour.

The structure of the paper is as follows. In Section 2, we discuss the cladding mechanical behaviour and its relation to viscoelasticity. The simulation model is constructed the Section 3 and its behaviour is investigated in Section 4. The results of the paper are discussed in Section 5 and summarized in Section 6.

2. Background

2.1. Mechanical response

The material response to stresses is usually a combination of elastic, viscous and plastic deformations. For metals the usually considered responses are elastic and viscoplastic (creep) responses. Historically, the cladding creep has been considered to follow the strain hardening law. This was shown by Lucas and Pelloux [1] to provisionally apply to Zircaloy-2 cladding. While their work also showed that the strain hardening rule does not hold for load drops and reversals (further corroborated by Matsuo [2]) many models have adopted it for taking stress transients into account. The online measurements of in-pile creep experiments at Halden reactor [3,4,8] show primary creep reinitializing at every stress change independent of accumulated strain and being proportional to the preceeding stress change, which also is at odds with the strain hardening rule.

Stress relaxation at the imposed specimen elongation is another difficult behaviour for strain hardening law to handle. In a stress relaxation experiment the highest stresses are encountered when the deformation is applied, and then the stresses reduce as the elastic deformation turns into plastic deformation. The strain hardening law assumes that at given stress the creep behaves as in the experiments with a single increase to the given stress. The law assumes that the change in stress can be dealt by moving to the creep curve corresponding to the new stress while keeping the strain constant. In the constantly diminishing stress case this means that all the changes advance the apparent time towards the steady state creep region. Effectively in a stress relaxation experiment nearly all of the deformation would be accounted for by the steady state creep, as the initial high stress provides enough strain for lower stress primary creep to saturate.

Historically the results obtained from stress relaxation experiments have been successfully used to obtain information on cladding creep properties of Zircaloy-2 and Zr-2.5 Nb samples in the region where creep stress dependency is linear, which was defined by the authors of the experimental papers as the region of less than 150 MPa of stress [9,10]. These stresses are encountered after the initial fast relaxation, and it is implicitly assumed that all the transient behaviour similar to primary creep has already happened during the loading of the sample and the initial fast relaxation. More recently there have been studies [11,12] showing that by increasing the stress exponent in creep correlations originally derived from creep experiments of Matsuo [13], the loading and initial relaxation of ZIRLO segments can be also described. However in these studies it is assumed that all the cladding behaviour can be described with equations originally describing only the steady state behaviour, which is curious considering the transient nature of the stress relaxation experiments. There are also other interpretations to the Zircaloy-4 stress relaxation results, such as dividing the stresses into transient and remnant [14], but these do not have direct correspondence to creep experiments.

Formulations of increasing complexity for describing the exact state of cladding do exist, e.g. Refs. [15,16]. Of interest here is the work of Delobelle et al. [15] where a complex model with kinematic variables is created. They concentrate on describing the anisotropy of the material and intentionally leave the description of anelastic properties from the model. However they note that its inclusion would be warranted to describe the cladding response to changing temperature. The model created is still considered too calculationally intensive for use in fuel performance codes [17] so there is still demand for the simplifying approach.

2.2. Viscoelastic modelling

Several authors have either described observed anelastic contributions [10,18] to cladding mechanical behaviour or used anelastic components as a part of their creep model [19]. In the following we use the terminology as defined by Nowick (p. 3 of [20]) where anelasticity is defined as time-dependent recoverable and viscoelasticity as time-dependent nonrecoverable mechanical behaviour. While the model we construct will contain an anelastic part, the inclusion of permanent deformation or steady state creep will make the model as a whole viscoelastic in nature.

Anelastic deformation is originated from several sources. According to Blanter et al. [21] these are point defects such an interstitial atoms which move or rotate in response to stresses to new positions, dislocations that move to accommodate the external stresses and interfaces of the larger scale structures such as grain boundaries, and the relaxation may originate from grain boundary sliding or movement in normal direction (grain growth). Thermoelastic relaxation also produce anelastic deformation as spatially heterogeneous thermoelastic stresses produce temperature gradients that relax by heat flow. Some of these mechanisms are accounted for in the mechanistic formulations of the creep, such as the build-up of internal stresses by pinning of dislocations. Yet in practice this has led to ignoring the anelastic component in engineering models. Therefore the separation of creep and anelastic deformation is warranted in a phenomenological formulation.

In metals anelastic strain is often considered small in relation to the other strain contributions. Also, in the usual applications, anelastic response operates in parallel with primary creep [22], and thus its effect is in part included in the primary creep formulations. However as anelastic deformation is both recoverable and time-dependent it can influence fuel cladding under changing conditions. While there are exceptions [19], not taking anelastic response into account can be considered as a norm in fuel behaviour code creep models.

In studies of viscoelastic properties of solids, a common method of describing models is via so-called mechanical analogs. These combine springs representing the elastic component of the material to dashpots representing the viscous components. The springs' displacement is $\varepsilon_{\text{spring}}=\sigma/\kappa_i$, where κ_i is the elastic modulus of spring i and σ is the external stress affecting the given component, while the dashpots' rate of displacement is of $\dot{\varepsilon}_{\text{dashpot}} = \sigma/\eta_i$, where η_i is the viscosity of the dashpot i.

A Kelvin unit is an analog with a spring and a dashpot in parallel. A general Kelvin model is a serial arrangement of n Kelvin units and a spring, as depicted in Fig. 1. The individual Kelvin units model various relaxation processes that take place at different time scales. The strain response to N step stress increases $\Delta\sigma_j$ at times t_j is [6].

$$\varepsilon(t) = \frac{\sigma(t)}{\kappa_0} + \sum_{j=1}^{N} \Delta\sigma_j \sum_{\kappa_i}^{1} \left(1 - e^{-\frac{t-t_j}{\tau_i}}\right) \Theta(t - t_j), \tag{1}$$

where κ_0 is the elastic modulus of the lone spring, κ_i is the elastic modulus of the spring of the ith spring-dashpot system, $\tau_i=\eta_i/\kappa_i$ is

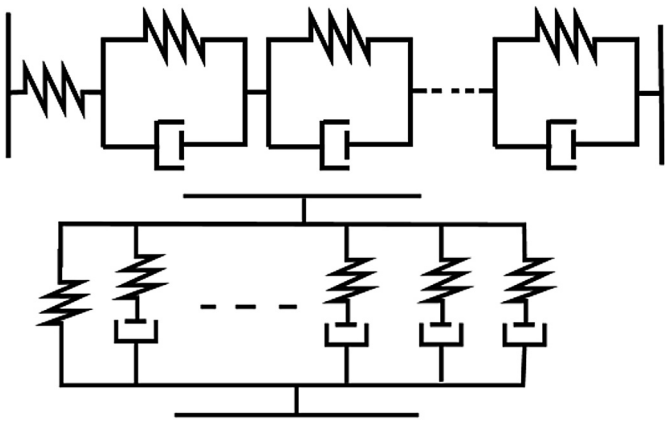

Fig. 1. Mechanical analog for the general Kelvin model (top) and the general Maxwell model (bottom).

the characteristic relaxation time of ith spring-dashpot system and Θ is the Heaviside step function. Higher n provides more accurate representation of a system with multiple relaxation modes at the cost of increasing model complexity. It should be noted that the individual Kelvin units are not meant to represent individual physical processes but instead a macroscopic aggregate of various microscopic processes acting on similar time scales.

The General Kelvin model is often used to analyse cases where the stress is a known input as the stress is transmitted along the whole system as per force balance and the solution of individual Kelvin units are separable. In cases where the imposed elongation is known, the general Maxwell model, consisting of parallel arrangement of a spring and n Maxwell units (a spring and a dashpot in series) is used instead. For both general models setting $n = 1$ creates a Standard Linear Solid (SLS) model (see e.g. pp. 87–88 of [23]).

3. Model for cladding mechanical response to transients

Usually the choice between Kelvin and Maxwell formulations is done based on the topic investigated. Our aim is to construct a model capable of simulating both creep and stress relaxation. We will also need to model the steady state creep, and this has been accomplished earlier [5,6] with a dashpot-like element placed in series to the rest of the solution. The steady state creep dashpot is decoupled from the rest of the solution in the imposed stress case but affects it in the imposed strain case. Therefore we can still obtain the "pure" solution to the general Kelvin model in the creep simulations while no such advantage can be had with the general Maxwell model. Therefore the former is chosen as a basis for our model.

The special case of the general Kelvin model with $n = 1$ units yields exponential time evolution, i.e. $e^{-t/\tau}$ for the viscoelastic deformation or primary creep. For zirconium alloy claddings, the time evolution of primary creep has been argued to be of the form $e^{-\sqrt{t}}$ [13,24] or a more complex one [19]. The $e^{-\sqrt{t}}$ form in particular is an instance of a stretched exponential or Kohlrausch function [25,26], which describes a system with several relaxation mechanisms operating at different rates. The stretched exponential can be approximated by a Dirichlet-Prony series (a weighted sum of exponential functions) [27]:

$$e^{-(t/\tau)^{\beta}} \approx \sum_{i=1}^{n} g_i e^{-t/\tau_i} \tag{2}$$

where each instance of e^{-t/τ_i} describes a relaxation mechanism with a time constant of τ_i and weight of g_i where $\sum g_i = 1$. This is the mathematical background justifying use of general Kelvin models with $n>1$ to describe the systems with observed time evolution of the type of Eq. (2).

We build a model with a spring for elastic response, n number of Kelvin units and a dashpot for plastic deformation, all in series. While conventionally the plastic deformation includes the primary creep, in this model the primary creep is as a whole given by the Kelvin units. This is in line with observed in-reactor creep behaviour [4–6,8]. In general the higher the model's n the better the description. However this both increases the complexity of the model and sets requirements for the amount and quality of the experimental data. In this work we restrict the model to n=1,2. For $n = 1$ this corresponds to our earlier modified SLS model [6]. The system for n=2 is displayed in Fig. 2.

The number of components in a system as depicted in Fig. 2 as well as nonlinearity of the most plastic deformation correlations makes finding analytical solution to the system challenging. A common engineering solution [7] is to use the internal variable approach, where the elongation of each individual component is calculated.

For stress relaxation, we use an explicit numerical solution, calculating the stress arising from the elastic deformation of the lone spring based on the difference between the imposed elongation and the elongation of Kelvin units and the lone dashpot as per Eq. (3). This stress determines the system stress as a whole. Then the elongations of the Kelvin units and the lone dashpot are calculated assuming the stress stays constant for the duration of the time step. The elongations of the Kelvin units are calculated based on Eq. (4) and the plastic strain from Eq. (5):

$$\sigma(t) = \left(\varepsilon_{tot}(t) - \varepsilon_s(t) - \sum_{i=1}^{n} \varepsilon_i(t)\right)\kappa_0, \tag{3}$$

$$\varepsilon_i(t+\Delta t) = \varepsilon_i(t) + (\sigma(t) - \varepsilon_i(t)\kappa_i)\cdot\left(1 - e^{-\frac{\Delta t}{\tau_i}}\right)\kappa_i^{-1}, \tag{4}$$

$$\varepsilon_s(t+\Delta t) = \varepsilon_s(t) + f(\sigma(t))\cdot\Delta t, \tag{5}$$

where ε_{tot} is the total (imposed) strain, κ_0 the elastic spring constant, ε_i, κ_i and τ_i are the strain, spring constant and characteristic time of the ith Kelvin unit, ε_s is the plastic strain, Δt the time step used and σ the stress. $f(\sigma)$ denotes the function for steady state creep rate, which may be a simple function of stress as will be used in this work or a more complex function such as the ones used by Matsuo [13] or Limback and Andersson [24]. This solution scheme requires using very short time steps.

For solving the system during imposed stress (creep experiment), Eqs. (4) and (5) can be directly used as the stress σ is known and each Kelvin unit as well as the lone spring and the lone dashpot experiences the same stress. In order to find out the strain of the

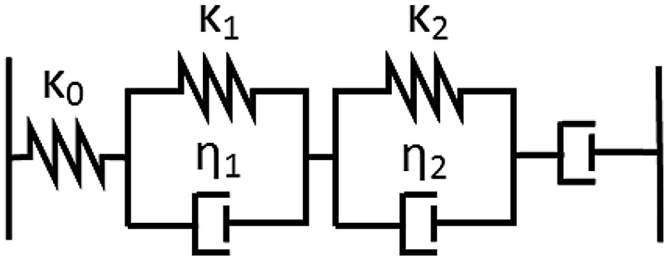

Fig. 2. Mechanical analog for the model describing cladding mechanical response containing a series of spring, 2 K units and a dashpot representing plastic deformation.

whole system ε_{tot} the individual strain components are combined:

$$\varepsilon_{tot}(t) = \frac{\sigma(t)}{\kappa_0} + \varepsilon_s(t) + \sum_{i=1}^{n} \varepsilon_i(t). \quad (6)$$

For the simulations initial values for the internal strains ε_i are needed. In this work we assume $\varepsilon_i(0)=0$ for the *laboratory conditions*. Validity of this assumption could be tested with annealing test of as-manufactured sample with zero externally applied stress. The experimental study with pressurized tubes published by Garzarolli et al. [28] would indicate that for the *reactor conditions* $\varepsilon_i(0) \neq 0$.

4. Model behaviour

4.1. Qualitative behaviour

We investigate the qualitative behaviour of two models, one with elastic (instantaneous recoverable deformation) and plastic (slow nonrecoverable deformation) components and the other with elastic, anelastic and plastic components. The former model corresponds in behaviour to traditional strain hardening models in situations where enough strain has been accumulated for the primary creep to be fully developed. The anelastic component is modelled with a single Kelvin unit yielding slow recoverable deformation, whereas the elastic and plastic components are the same in both models.

One technique for investigating the metal transient response is called stress dip experiment (e.g. p. 67 of Ref. [22]). In the experiment a load is first applied to a sample until a steady strain rate is achieved. Then, the load is reduced for a while and finally increased to its original value. According to Ref. [22], the sample deformation appears to stop for a while at the load reduction before it starts to creep at the rate corresponding to the reduced stress. After the subsequent increasing of the stress the strain rate increases for a while before returning to the strain rate corresponding to the applied stress. Models based on purely plastic deformation do not explain these observations, but as illustrated in Fig. 3a, the observed behaviour is well in line with the one provided by the viscoelastic model.

Several authors of experimental papers [24,29] describe issues encountered when during a creep experiment the stress is reduced to zero while the sample is still at the experimental temperatures. Limback and Andersson [24] describe the need to quickly cool down the experimental Zircaloy-4 sample before the creep recovery sets in and Kozar et al. [29] measure the change in strain in Zircaloy-2 samples during zero stress period. Fig. 3b shows the difference between traditional and viscoplastic interpretation following a prolonged zero stress period. It should be noted that it is common to clean up such periods of zero stress from experimental results, as according to strain hardening law they should not have any effect on the sample strain. However, this results in fast dips in measured strain, which is subsequently recovered, as seen for instance in Fig. 3 of Kozar et al. [29].

Kapoor et al. [14] have performed stress relaxation experiments where they attempt to expedite the acquisition of what they call remnant stress (stress remaining after a long time from the beginning of the stress relaxation experiment) by stepwise reduction of imposed elongation. They report observing at some occasions that after the elongation reduction the stress of the sample increases, contrary to what the plastic models would indicate. As demonstrated in Fig. 3c this can be explained by the viscoelastic properties of the material. The plot also shows that the addition of viscoelastic component to mechanical model increases the rate of initial stress relaxation.

Finally, in Fig. 3d, the strain recovery annealing experiment is illustrated. While the rate of stress relaxation depends on the assumed plastic strain rate, one definite viscoelastic effect can be demonstrated. At the end of the stress relaxation experiment when the loading device is relaxed, i.e. no elongation is imposed and the stress of the sample is at zero, the viscoelastic deformation continues if the elevated temperature is maintained. Should the deformation be purely plastic no deformation should be seen after the load is removed. The same effect can be obtained with post test annealing of the samples. Such observations of strain recovery annealing are reported by Causey et al. [10] who describe it being anelastic in nature.

4.2. Quantitative behaviour

In order to demonstrate the model capability to describe both creep and stress relaxation behaviour, we need experimental data on both experiment types performed on similar samples. These are surprisingly hard to find from open literature, as most of the experimental publications focus on either creep or stress relaxation experiments. As the cladding mechanical properties are strongly influenced by the manufacturing processes and the final heat treatment, the different samples require different model parameters.

Delobelle et al. [15] performed various experiments, including both creep and stress relaxation, for unirradiated Zircaloy-4 samples with two different experimental heat treatments. As they performed both experiments using similar samples we can use the creep experiment to determine the required material-dependent coefficients for our model and use them to simulate the stress relaxation experiment. While Ref. [15] provides a wealth of experimental data, most of it focuses on investigation of material anisotropy. In this work we use the available uniaxial data from the publication, which concerned the experiments in the axial direction for both the recrystallized (denoted by Denobelle et al. as the R sample) and the cold worked stress relieved (denoted by Denobelle et al. as the CWSR sample) Zircaloy-4 at 623 K (350 °C). The former state was achieved with a thermal treatment of 4–5 h at 973 ± 30 K and the latter with 5 h at 733 K. The data for creep experiment was taken from Fig. 16 of Ref. [15] and for stress relaxation from Fig. 15 of Ref. [15]. As all the experiments discussed in this work have been performed at the same temperature, we can focus on the mechanical response of the material.

In the creep experiments the stress was stepwise increased and the elongation measured. For R sample the stress steps used were 125, 135, 150 and 170 MPa and for the CWSR sample 170, 250 and 300 MPa. In the stress relaxation experiments the sample was deformed to a desired strain at the rate of $6.6 \cdot 10^{-4}$ s^{-1}. Then the strain was held constant for 48 h and the stress measured. The strain steps were 0.4%, 0.8%, 1.2%, and 4% for the R sample and 0.4%, 0.8%, and 1.2% for the CWSR sample, with the original zero strain kept as a reference level during the experiment.

Delobelle et al. [15] provide measured Young's modulus for both R and CWSR samples ($7.8 \bullet 10^4$ MPa and $7.3 \bullet 10^4$ MPa, respectively). These are relatively close to the MATPRO [13,24,30] formula

$$E = 1.148 \cdot 10^5 - 59.9T \text{ MPa}, \quad (7)$$

where T is temperature in K, giving $E=7.7482 \cdot 10^4$ MPa at 623 K. The reported value is used for the CWSR material. However, the R material appears to be extremely soft so that in order to use the reported value for Young's modulus and match the experimental observations we would need to assume very rapid deformation after the initial elastic jump. In the following the rapid deformation is combined with the elastic response, represented by the apparent

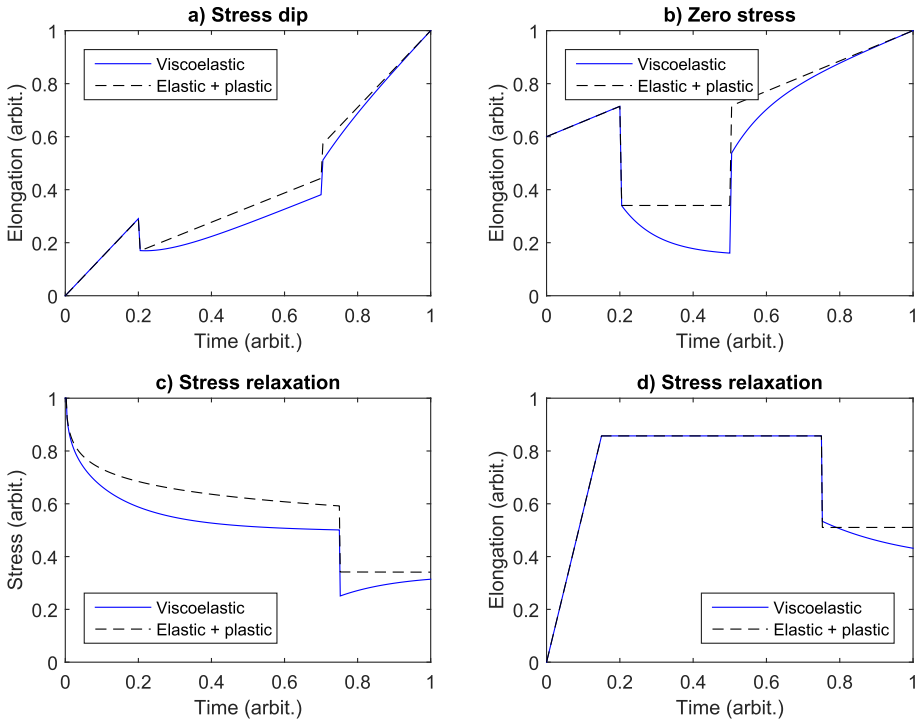

Fig. 3. Qualitative behaviour of viscoelastic model as compared to model with purely elastic and plastic components. The solid line denotes the viscoelastic model results and the dashed line a corresponding model with only elastic and plastic components. In the simulation shown in the upper left plot (a), the sample stress has first been held until steady state creep has been obtained. Then the stress is reduced for a while, and returned to its original value. The viscoelastic model shows apparent stop at stress dip, and faster elongation at return to stress. The upper right plot (b) features similar situation, but with the stress reduced to zero. The apparent deformation continues in viscoelastic model, but will return to in line with the previously achieved rate as is seen in several experiments [24,29]. The lower left plot (c) features a stress relaxation experiment where the elongation is reduced mid-experiment as per Ref. [14]. The viscoelastic model shows in this particular case an increase in stress as reported. In the lower right plot (d) the stress relaxation experiment ends with a release of the sample, yielding σ=0 at the last part of the plot. This causes a viscoelastic deformation that is not seen if the sample deformation is assumed to consist of solely elastic and plastic components.

Young's modulus of $3.9\cdot10^4$ MPa, as the coarse experimental data does not allow us to differentiate between them. This effectively reduces the maximum stresses in the stress relaxation predictions.

We use a simple engineering model for the modelling of the steady state creep:

$$\dot{\varepsilon}_t = A\sinh(B\sigma), \tag{8}$$

where A and B are coefficients fitted to the steady state creep data obtained from Fig. 6 of [15]. The coefficients are listed in Table 1 and the steady state creep rate provided by Eq. (8) as a function of applied stress is shown in Fig. 4. The use of hyperbolic sine function is a common engineering approximation used to cover both low stress region below 100 MPa where $\dot{\varepsilon} \sim \sigma$ and high stress region where $\dot{\varepsilon} \sim \sigma^5$ [31,32]. At high stress limit the hyperbolic sine tends to exponential behaviour, which is in line with power law break down region.

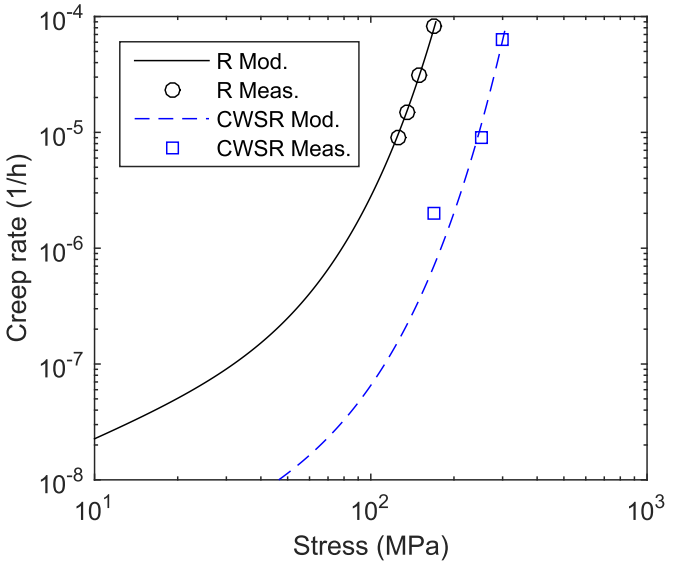

Fig. 4. Steady state creep rate for R and CWSR claddings as a function of applied stress. Lines represent model results and circles and squares values calculated from experimental data. Experimental data obtained from Fig. 6 of [15] and simulated rates as per Eq. (8).

The first stress step is simulated for the creep experiment and the model parameters are fitted to match the experimental data. Creep experiments have been successfully modelled earlier with a $n = 1$ model [5,6], and a $n = 2$ model will be used to investigate the effect of increasing the number of Kelvin units. For the individual Kelvin units the strength of the springs (κ_i) determine the extent of the elongation in creep experiments and the characteristic time is determined by $\tau_i = \eta_i/\kappa_i$. For the model with $n = 1$ both κ and τ are fitted to the creep experiments. For the model with $n = 2$ we use τ_1 to correspond to the fast and τ_2 to the slow creep compliance, assuming $\tau_2 = 10\tau_1$ to limit the number of free variables and obtain a clear separation of effect of individual Kelvin units, and use Matlab optimization tools to fit the curves to the creep experiments. The resulting coefficients are listed in Table 1. The stress transient in the creep experiment is assumed to be instantaneous.

For the stress relaxation experiment all the experimental strain steps were modelled. During the periods where the strain was increased to new holding level several steps of the strain increase were modelled. In most of the cases this resulted in maximum

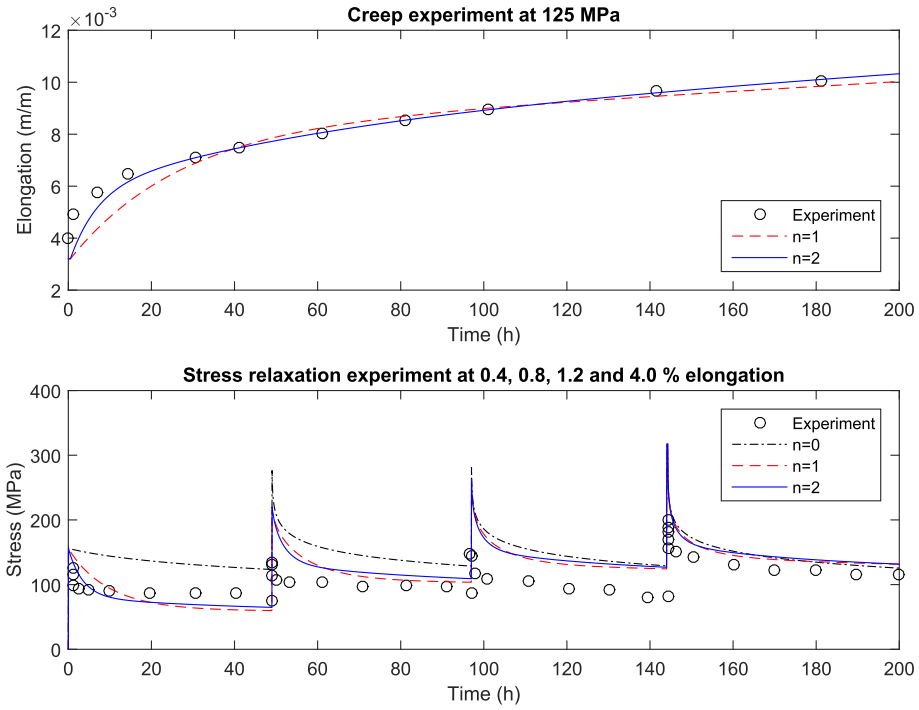

Fig. 5. Creep and relaxation of R samples. Comparison between the experimental data (circles) and simulations with model with different number n of Kelvin units. $n = 0$ represents the pure elastic and plastic deformation, $n = 1$ is the Standard Linear Solid and plastic deformation, $n = 2$ the model introduced in this paper.

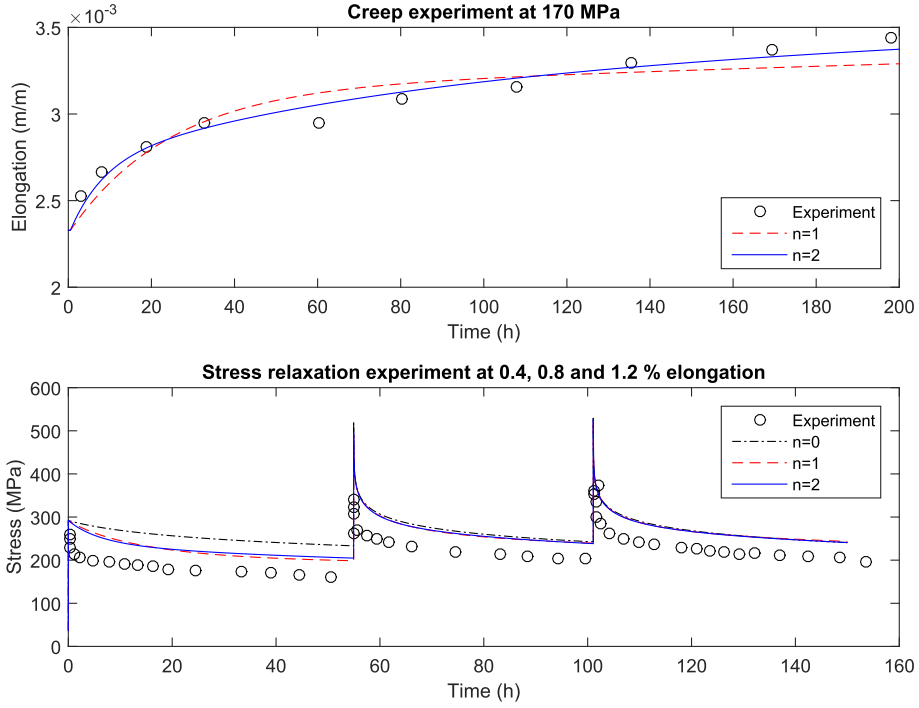

Fig. 6. Creep and relaxation of CWSR samples. Comparison between the experimental data (circles) and simulations with model with different number n of Kelvin units. $n = 0$ represents the pure elastic and plastic deformation, $n = 1$ is the Standard Linear Solid and plastic deformation, $n = 2$ the model introduced in this paper.

stress reduction of less than 5 MPa when compared to instantaneous strain. As the strain was applied at the rate of $6.6 \cdot 10^{-4}$ s^{-1} yielding strain of 0.4% in approximately 6 s, the small difference between instant and very fast strain increase is understandable. The exception was the last step of the R sample (to 4% strain) where the strain increase was high enough to require taking the relaxation into account during the increase.

The simulation of the creep and stress relaxation experiments are shown in Fig. 5 for R samples and in Fig. 6 for the CWSR samples. The simulations are performed with models with 0, 1 and 2 Kelvin units. The model with 0 Kelvin units is shown only for the stress relaxation plot, where it represents the traditional strain

Table 1
Model coefficients used to model both R and CWSR claddings.

Cladding	A (1/h)	B (1/MPa)	κ_0 (MPa)	κ_1 (MPa)	κ_2 (MPa)	τ_1 (h)	τ_2 (h)
R $n=0$	4.5168×10^{-6}	4.82×10^{-2}	3.9×10^{4}	–	–	–	–
R $n=1$	4.5168×10^{-6}	4.82×10^{-2}	3.9×10^{4}	2.52×10^{4}	–	26	–
R $n=2$	4.5168×10^{-6}	4.82×10^{-2}	3.9×10^{4}	4.80×10^{4}	4.49×10^{4}	6.5	65
CWSR $n=0$	4.2416×10^{-7}	3.43×10^{-2}	7.3×10^{4}	–	–	–	–
CWSR $n=1$	4.2416×10^{-7}	3.43×10^{-2}	7.3×10^{4}	2.08×10^{5}	–	24	–
CWSR $n=2$	4.2416×10^{-7}	3.43×10^{-2}	7.3×10^{4}	4.40×10^{5}	3.03×10^{5}	8.0	80

hardening law model in stress relaxation, as discussed in Section 2.

5. Discussion

The anelastic contribution to cladding mechanical behaviour has been investigated and accounted for in some models in the 1970s and 1980s [10,18,19]. However, later on it has been neglected [1,2,15,24], either implicitly or explicitly, and several experimentally observed cladding transient responses have remained unexplained. Yet the viscoelastic model described in this paper is able to provide a qualitative interpretation of the observations on the metal response to transient stresses such as load drops, creep reversal and quick stress relaxation. The observed time evolution of the primary creep can be explained by various concurrent processes operating at different time scales and approximated by a series of relaxation processes. In our previous work we have shown that similar models can be used to simulate various creep experiments performed both in laboratory conditions and in-pile [5,6]. The model is self consistent in the sense that the creep and stress relaxation are simulated with the single model.

Figs. 5 and 6 show the benefit of inclusion of Kelvin units to the simulation model, as both the creep and stress relaxation modelling is improved. While the creep results with the model without anelastic contribution (n=0) would not represent traditional models as there is no primary creep contribution, with the stress relaxation it provides the results corresponding to the use of strain hardening law. Increasing the number of Kelvin units enhances the correspondence between the measurements and the simulation results. This is especially noticeable in stress relaxation of R sample in Fig. 5. However, the stress relaxation experiments also demonstrate the current shortcomings of the model. The stresses, especially the maximum ones, are generally overestimated. The time evolution of the model, while qualitatively correct, is still somewhat too slow. However, for the uniaxial creep and stress relaxation, the simple model presented in this paper performs similarly to the one derived by Delobelle et al. [15].

The maximum stresses are encountered when the strain has reached the target value. They are overestimated by our model as well as the model used by the authors of the original experimental paper [15]. The stress given by the model is dominated by the elastic modulus of the material. Delobelle et al. [15] assume the reason is that during the imposing of the strain the sample plastically deforms. This is probable as the strain rate is high enough to require very fast relaxation processes if the instantaneous plastic deformation is ruled out. However there is not enough experimental data to create a strain rate dependent plastic deformation model.

The modelling of especially R specimen could be improved by using higher n to simulate a larger range of time dependent processes. However, as the data available are just a few points, that is not feasible within this work. Also, it should be noted that the current implementation presented in Eqs. (3)–(5) requires the use of time steps shorter than the smallest τ_i in the stress relaxation simulations. This limits the n to be used in an actual fuel performance application.

The comparison of Figs. 5 and 6 demonstrates that the creep strength of the material also has an effect on whether taking viscoelastic effects into account is necessary. The viscoelastic contribution to creep resistant CWSR specimen is small and this shows in the stress relaxation experiment. On the other hand in the soft R specimen the viscoelastic contribution is visible in both the creep and stress relaxation experiments. It should be noted that in-pile conditions appear to enhance the viscoelastic contribution [10] and it is not affected by the accumulated fluence according to the observations in the instrumented creep experiments performed at Halden reactor [4,8].

It should be also noted that in the stress relaxation experiments the viscoelastic behaviour has most effect on the first relaxation. This stems from the assumptions made in the model. First, initially the sample is assumed to be relaxed to zero stress, yielding the stress differential of 200–300 MPa depending on material at the start of the experiment. At subsequent strain jumps this difference is somewhat smaller. And while the viscoelastic part is assumed to be linear and to operate on the stress difference, the plastic part of the model depends on the stress and is strongly non-linear in the region of the later strain steps.

6. Conclusions

Accurate modelling of nuclear fuel cladding mechanical behaviour is important for both fuel performance and safety analysis. The mechanical response to transient stresses has traditionally been analysed as consisting of elastic and (visco)plastic components, with the latter containing all non-instantaneous phenomena. Usually the changing conditions have been taken into account by strain hardening rule, which is an engineering approximation assuming accumulated creep strain stays invariant when the conditions change. Historically the anelastic contribution to nuclear fuel cladding mechanical behaviour has been identified. However for some reason it has not been taken into account in the models currently in use in nuclear fuel behaviour analysis. This has lead to the inability to explain several experimental observations such as re-initiation of in-pile primary creep.

In this paper we have derived a model for describing both the creep and the stress relaxation using the methods from the theory of viscoelasticity. An appropriate model formulation has been designed based on the application, and its ability to model cladding mechanical transients has been demonstrated. Also, an interpretation on the observed time-dependence of the primary creep evolution has been provided. Based on the analysis presented we argue that the inclusion of anelastic contribution to the cladding mechanical models provides a simple way to improve the simulation results. While the effect is most pronounced at small strain jumps and low stress situations, it should be noted that both slow strain rates and reactor conditions can be expected to make the viscoelastic effects more important.

The ultimate goal of the research presented is a creation of a cladding mechanical model both capable of consistent description

of creep and stress relaxation behaviour and implementable to a fuel behaviour code. The remaining major methodological challenges are the cladding response to the changes in temperature and the correspondence between the in-pile and the out-of-pile cladding behaviour. These, along with the validity of the assumption made in this work that the anelastic part of the model is initialized at rest, are to be investigated in the future.

Acknowledgements

This work was partially funded by SAFIR2014, the Finnish Research Programme on Nuclear Power Plant Safety 2011-2014, and Academy of Finland funded IDEA project (grant decision number 260493).

References

[1] G. Lucas, R. Pelloux, Nucl. Technol. 53 (1981) 46–57.
[2] Y. Matsuo, ASTM STP 1023 (1989) 678–691.
[3] M. McGrath, in: Proceedings of the 2000 International Topical Meeting on LWR Fuel Performance, 2000.
[4] J. Foster, M. McGrath, in: Proceedings of the 2007 LWR Fuel Performance Meeting, 2007.
[5] V. Tulkki, T. Ikonen, J. Nucl. Mater. 445 (2014) 98–103.
[6] V. Tulkki, T. Ikonen, J. Nucl. Mater. 457 (2015) 324–329.
[7] H. Banks, S. Hu, Z. Kenz, Adv. Appl. Math. Mech. 3 (2011) 1–51.
[8] S. Hanawa, HWR-882, 2008.
[9] D. Fraser, P. Ross-Ross, A. Causey, J. Nucl. Mater. 46 (1973) 281–292.
[10] A. Causey, F. Butcher, S. Donohue, J. Nucl. Mater. 159 (1988) 101–113.
[11] Y. Long, C. Beard, S. Henk, G. Zhou, in: Proceedings of 2010 LWR Fuel Performance Meeting, 2010. Paper 054.
[12] G. Zhou, L. Hallstadius, G. Wikmark, Y. Long, J. Foster, in: Proceedings of 2011 Water Reactor Fuel Performance Meeting, 2011. Paper T2–038.
[13] Y. Matsuo, J. Nucl. Sci. Technol. 24 (1987) 111–119.
[14] R. Kapoor, S. Wadekar, J. Chakravartty, Mater. Sci. Eng. A 328 (2002) 324–333.
[15] P. Delobelle, P. Robinet, P. Geyer, P. Bouffioux, J. Nucl. Mater. 238 (1996) 135–162.
[16] L. Jernkvist, in: Transactions of the 15th International Conference on Structural Mechanics in Reactor Technology (SMiRT-15) C04/3, 1999, pp. 477–484.
[17] M. Rautenberg, D. Poquillon, P. Pilvin, C. Grosjean, J. Cloue, X. Feaugas, Nucl. Eng. Des. 269 (2014) 33–37.
[18] F. Povolo, B. Molinas, J. Nucl. Mater. 114 (1983) 85–94.
[19] K. Murty, K. Yoon, in: Transactions of the 5th International Conference on Structural Mechanics in Reactor Technology (SMiRT-5) C3/6, 1979.
[20] A. Nowick, B. Berry, Anelastic Relaxation in Crystalline Solids, Academic Press, New York, 1972.
[21] M. Blanter, I. Golovin, H. Neuhuser, H. Sinning, Internal Friction in Metallic Materials: a Handbook, Springer, 2007.
[22] F. Nabarro, F. de Villiers, Physics of Creep and Creep-resistant Alloys, CRC Press, 1995.
[23] D. Gutierrez-Lemini, Engineering Viscoelasticity, Springer, 2014.
[24] M. Limback, T. Andersson, ASTM STP 1295 (1996) 448–468.
[25] R. Kohlrausch, Pogg. Ann. Phys. Chem. 91 (1854) 179.
[26] R. Anderssen, S. Husain, R. Loy, Anziam J. 45 (2004) C800–C816.
[27] R.S. Anderssen, M.P. Edwards, S.A. Husain, R.J. Loy, in: 19th International Congress on Modelling and Simulation, 2011, pp. 263–269.
[28] F. Garzarolli, H. Stehle, E. Steinberg, ASTM STP 1295 (1996) 12–32.
[29] R. Kozar, A. Jaworski, T. Webb, R. Smith, J. Nucl. Mater. 444 (2014) 14–22.
[30] W. Luscher, K. Geelhood, NUREG/CR-7024, 2011.
[31] T. Hayes, M. Kassner, R. Rosen, Metallurgical Mater. Trans. A 33A (2002) 337–343.
[32] T. Hayes, M. Kassner, Metallurgical Mater. Trans. A 37 A (2006) 2389–2396.